Subcritical crack growth in silicon carbide

K. D. McHENRY, R. E. TRESSLER
Department of Materials Science, The Pennsylvania State University, University Park, Pennsylvania, USA

Crack growth behaviour in two types of commercially available silicon carbide was examined from 600 to 850° C in ambient atmospheres containing oxygen, water vapour, and sulphur dioxide. The double-torsion specimen was used in the incremental displacement rate mode to yield (K_1, V) relations. The direct-bonded material exhibited unstable crack propagation and arrest behaviour which was not measureably affected by temperature variations or the corrosive environments. The hot-pressed material exhibited subcritical crack growth similar to the three regions of the classical (K_1, V) diagram. Oxidation of the silicon carbide is suggested to be the mechanism of stress corrosion operating in these environments.

1. Introduction

Subcritical crack growth has been well documented in oxide ceramics such as glasses [1–5] and alumina [4] for a range of temperatures and environments. The crack velocity results have generally shown three regions of behaviour as the stress intensity factor increases: region I bounded by the fatigue limit at low K_Is with the crack velocity controlled by the rate of the stress corrosion reaction; region II in which the velocity is nearly constant with increasing K_I and thought to be controlled by delivery rate of corrosive species to the crack tip; and region III in which the crack velocity increases rapidly with K_I approaching K_{IC}, and is thought to be controlled by factors intrinsic to the material. Relatively little work has been conducted on the mechanisms of subcritical crack growth in silicon carbide ceramics, which are being considered for high performance applications in severe environments. To date, crack growth data for hot pressed silicon carbide are available for environments of toluene, argon, and water at room temperature [6, 7], at 600° C [7] and 1400° C in air [7, 8], and for sintered silicon carbide as well as hot-pressed silicon carbide at 1600° C in air [8]. The results of Evans and Lange [7] and the present authors [6] have shown the existence of moisture-induced stress corrosion in hot-pressed silicon carbide near room temperature. The value of the slope in the Region I portion of the (K_I, V) diagram, the region of slow crack growth controlled by stress corrosion, is ~100, indicating that the mechanism of moisture-induced stress corrosion is not a serious consideration for life-time predictions since crack growth will not occur until K values approaching K_{IC} are realized in service.

Oxidation or corrosion can significantly affect the strength of silicon carbide. Oxidation reduces the room temperature bend strength of self-bonded SiC [9], but has almost no effect on the room temperature bend strength of hot-pressed SiC [10, 11], and increases the room temperature bend-strength of Crystar SiC [11]. The different behaviour of these materials has been attributed to the crack-healing ability of the oxidation products or the crack blunting associated with oxidation itself [12]. Other work [13] has shown that hot-pressed silicon nitride is stronger *in vacuo* than in air indicating that oxidation may have accelerated cracking.

2. Experimental procedure

2.1. Materials and characterization

The hot-pressed silicon carbide* and direct-bonded silicon carbide† were obtained from the Norton Company. Weaver and Olson [14] have reported

*NC203
†NC400, The Norton Company, Worcester, Mass, USA.

© 1977 Chapman and Hall Ltd. Printed in Great Britain.

the fabrication processes and the general properties for the hot-pressed silicon carbide. The material has a grain size of 2 to 5 μm and Al_2O_3 is added as a hot-pressing aid. Torti et al. [10] and Rogers [15] have reported a density of $2.6\,g\,cm^{-3}$ and an apparent porosity of 14% for the direct-bonded material. This material has a grain size of 100 to 200 μm. Edington *et al.* [12] have reported the presence of several per cent free silicon in the direct-bonded material.

The examination of fracture surfaces and determination of grain sizes were performed with a scanning electron microscope. The energy dispersive X-ray fluorescence analyser in the SEM was used to analyse for impurities and their spatial distribution. The polytypes of SiC were identified by X-ray diffraction analyses. Bulk densities were determined from sample weights and dimensions. The elevated temperature moduli were obtained by resonance techniques from room temperature to 800° C in air. The specimens were suspended from transducers with thin wires into a split-tube furnace. The flexural resonance frequency, necessary for the calculation of the elastic modulus, was monitored from room temperature to 800° C.

2.2. Thermogravimetric analysis

Thermogravimetric analyses were conducted in an attempt to correlate variations in corrosion behaviour with differences in stress-corrosion phenomena. The thermogravimetric analyses were conducted at 1000° C in argon, argon plus 1 vol% oxygen, argon plus 0.3 vol% water vapour, and argon plus 1 vol% sulphur dioxide. Argon which contained <0.5 ppm H_2O according to the supplier's specifications was used as the carrier gas with a flow rate of $300\,cm^3\,min^{-1}$.

The system was flushed with argon for approximately 20 min before each run to minimize the amount of residual oxygen and nitrogen in the system. All gases were passed through anhydrous $CaSO_4$ before entering the system to minimize additional H_2O impurities. After this step, the sulphur dioxide or oxygen was added. The water vapour was introduced by bubbling one half of the argon stream through water before entering the furnace chamber.

Samples for the analyses were small square plates having surface areas of 6 to $10\,cm^2$ as determined from the sample dimensions. The hot-pressed material was polished with 6 μm diamond paste before testing while the direct-bonded material was tested with the as-received surface intact. The resulting weight changes of the materials were monitored using an Ainsworth semi-micro recording balance from which the samples were suspended. The furnace was a vertical split-tube type controlled to ± 2° C with a Eurotherm controller.

2.3. Elevated temperature double torsion testing

The dimensions of the direct-bonded silicon carbide double torsion specimens were 3 in. × $1\frac{1}{4}$ in. × $\frac{1}{8}$ in. A very shallow groove, typically 0.01 in., was cut into these specimens to guide the crack. The dimensions of the hot-pressed silicon carbide double torsion specimens were 3 in. × $1\frac{1}{4}$ in. × 0.075 to 0.090 in. The thickness of the specimens in the groove was maintained at 0.030 to 0.040 in. The specimens were cut from the billet such that the specimen faces were perpendicular to the hot-pressing direction.

The high temperature testing was accomplished by the incremental displacement rate mode [4], where the stress intensity factor is given by:

$$K_I = PW_m\left[\frac{3(1+\nu)}{WD_nD^3}\right]^{1/2} \tag{1}$$

where K_1 is the stress intensity factor for mode I failure, P is the load, W_m is the moment arm, W is the width of double-torsion specimen, D is the thickness of double-torsion specimen, and D_n is the thickness of specimen remaining after grooving.

The crack velocity is given by:

$$V = \frac{\dot{y}}{BP} \tag{2}$$

where V is the crack velocity, $\dot{y}$ is the displacement rate, and B is the slope of the compliance curve. The values of K_{IC} were determined by rapidly loading a pre-cracked specimen to failure at a displacement rate of $0.1\,in.\,min.^{-1}$

The direct-bonded material was tested in argon plus 0.3 vol% water vapour, and argon plus 1 vol% sulphur dioxide at 800 and 600° C. The hot-pressed material was tested in argon plus 0.3 vol% water vapour at 850, 800, 750 and 600° C. Argon plus 1 vol% sulphur dioxide, argon plus 1 vol% oxygen, and "pure" argon were also used at 800° C. The procedure for introducing and treating the gases was similar to that used in the thermogravimetric analyses.

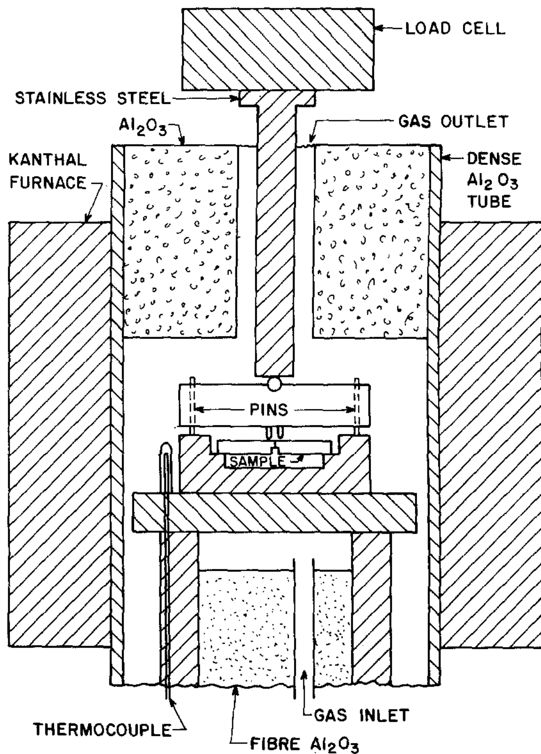

Figure 1 Schematic diagram of load train and furnace arrangement for elevated temperature double-torsion testing.

The load train and furnace arrangement used for testing is schematically shown in Fig. 1. For each investigation, the appropriate gas mixture was flushed through the system before the furnace was heated to the required temperature. The furnace hot zone was, vertically, ~ 2 in. with a temperature gradient across the sample of ± 1° C. Once the desired furnace temperature was attained, a small load, typically 1 to 2 lb, was applied and the whole system was allowed to equilibrate at that temperature. The sample was then loaded at a displacement rate of 0.002 in. min^{-1} until "pop-in" of the crack was observed by a rapid load drop. Following the "pop-in", different strain rates were used to obtain the various points on the (K_I, V) diagram. A table model Instron testing machine was used for all mechanical testing.

3. Results and discussions

3.1. Characterization

With the exception of moduli and Poisson's ratios, the results of the characterization of the hot pressed silicon carbide agree well with the results of Weaver and Olson [14]. The value of Poisson's ratio obtained in this investigation, 0.12, is much lower than reported previously, 0.17 [14].

The direct-bonded material has a grain size of 100 to 200 μm and an apparent porosity of 16%. The density was 2.65 g cm^{-3}, approximately 81% of the theoretical value. Aluminium was detected at the grain boundaries with the energy dispersive X-ray fluorescence analysis. Several per cent free silicon is also present. The elevated temperature moduli for the direct-bonded and hot-pressed materials are shown in Table I. The elastic modulus, E, was measured directly, Poisson's ratio was assumed to be constant over the temperature range (room temperature to 800° C), and the shear modulus, G, was calculated from:

$$\frac{E}{2G} - 1 = \nu. \tag{3}$$

3.2. Oxidation

The hot pressed material exhibited a maximum of 0.1 mg weight increase at 1000° C for all test environments. This magnitude of weight change approached the lower limit of resolution of the apparatus used. A small amount of oxidation did occur since interference colours could be seen on the samples upon removal from the furnace.

The results of the thermogravimetric analyses for the direct-bonded material are shown in Fig. 2. Table II lists the partial pressure of oxygen available in the system due to each of the conditions shown in Fig. 2.

TABLE I Elevated temperature elastic moduli of SiC

		27° C	400° C	600° C	800° C
Hot-pressed SiC	ν	0.115	0.115	0.115	0.115
	E	66.3×10^6 psi*	65.2×10^6 psi	64.8×10^6 psi	64.1×10^6 psi
	G	29.5×10^6 psi	29.4×10^6 psi	29.2×10^6 psi	28.9×10^6 psi
Direct-bonded SiC	ν	0.110	0.110	0.110	0.110
	E	35.1×10^6 psi	34.2×10^6 psi	34.0×10^6 psi	33.3×10^6 psi
	G	15.5×10^6 psi	15.4×10^6 psi	15.3×10^6 psi	15.0×10^6 psi

*10^3 psi = 6.89 N mm^{-2}.

TABLE II Available partial pressure of oxygen in the TGA furnace ambient calculated from gas phase thermodynamic data at 1000° C

Input environment	P_{O_2} (atm)
Ar	5.0×10^{-7}
Ar + 1 vol% O_2	2.99×10^{-3}
Ar + 0.3 vol% H_2O	1.54×10^{-6}
Ar + 1 vol% SO_2	5.56×10^{-6}

According to Singhal [16] the oxidation of silicon carbide is governed by the reaction:

$$SiC_{(s)} + \tfrac{3}{2} O_{2(g)} = SiO_{2(s)} + CO_{(g)}. \quad (4)$$

If the partial pressure of carbon monoxide in Equation 4 is fixed at 1 atm. or less, the calculated equilibrium partial pressures of oxygen in Equation 4 are less than the partial pressures of oxygen which were available in the system as given in Table II. This result indicates that the available partial pressures of oxygen are high enough so that oxidation to SiO_2 should occur at 1000° C.

Fig. 2 shows that as the partial pressure of oxygen is increased, the total amount of weight gained is increased. Nair *et al.* [17] have shown that increasing the oxygen pressure will cause an increase in the concentration of oxygen in the glass in equilibrium with the oxygen containing phase. Under the conditions represented in Fig. 2, as the partial pressure of oxygen is increased, the oxygen concentration at the surface of the product silica layer will increase. This increased concentration gradient results in more oxygen being

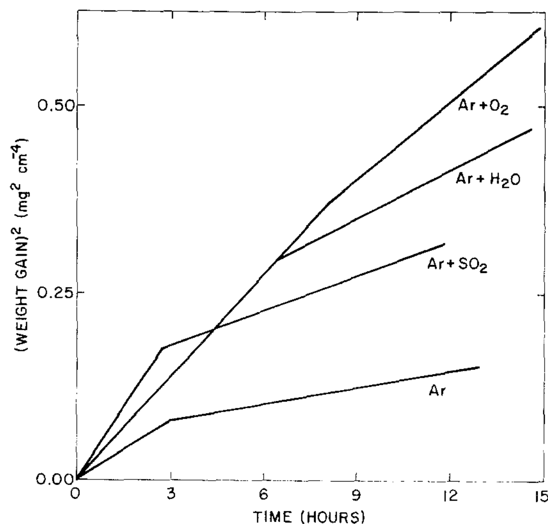

Figure 2 Thermogravimetric analyses of direct-bonded silicon carbide at 1000° C.

delivered to the SiO_2–SiC interface, causing an increased oxidation rate.

In addition to the total weight gain increasing with the partial pressure of oxygen, the parabolic oxidation rate also increases with the partial pressure of oxygen. This information in addition to the results of Nair *et al.* [17] indicate the diffusion of oxygen is rate-controlling for these oxidation studies.

The initial oxidation rates (up to about 3 h) shown in Fig. 2 are greater than the oxidation rates at 12 to 15 h. These high initial oxidation rates are probably due to the oxidation of the free silicon.

It has been reported in the literature [18] that water vapour increases the oxidation rate of silicon carbide. Fig. 2 alone does not indicate this. However, if the partial pressures of oxygen are considered, it is seen that the partial pressure of oxygen in the water vapour investigation is three orders of magnitude smaller than in the oxygen investigation. Thus, the water vapour may indeed have increased the oxidation rate over that which one would observe in a dry system with the same partial pressure of oxygen.

No weight loss was noted in any of the samples in any of the environments. This result, in addition to those of Lin [19] indicates that oxidation produces SiO_2 and not gaseous SiO which would result in loss of weight.

The oxidation of the direct-bonded material was more pronounced for two reasons. The first reason is that the surface area measured using sample dimensions was probably a gross underestimate of the actual surface area due to the large fraction of interconnected porosity in the direct-bonded material. Thus, the effective surface area is much larger than the calculated surface area. The second reason is the presence of free silicon which oxidizes more rapidly than SiC.

3.3 High temperature crack propagation results

The direct-bonded material exhibited unstable crack propagation and arrest behaviour at all temperatures and in all environments investigated. Upon loading a pre-cracked specimen, the crack front would erratically "pop-in" and arrest at low deflection rates with no continuous subcritical crack growth noted. The value of K_{IC} determined at higher deflection rates was reproducible at $2.09\,MN\,m^{-3/2}$. The unstable crack propagation and arrest behaviour in this material is attributed

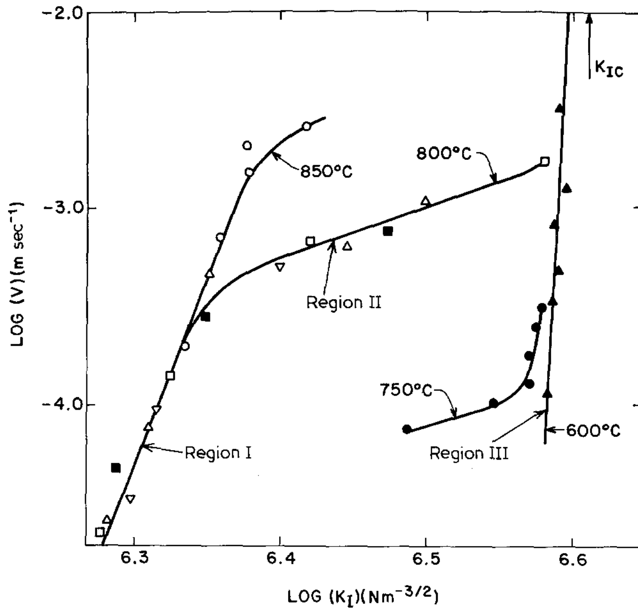

Figure 3 Stress intensity factor versus crack velocity for hot-pressed silicon carbide at elevated temperatures.

● 750° C	Ar + H_2O	▿ 800° C	Ar + O_2
□ 800° C	Ar + SO_2	■ 800° C	Ar
△ 800° C	Ar + H_2O	▲ 600° C	Ar + H_2O
○ 850° C	Ar + H_2O		

to the large grain size relative to the sample dimensions. The type of fracture observed was transgranular for all environments. Variations in the test temperature and gaseous environment did not affect the stress-intensity values for crack initiation and arrest.

The (K_I, V) data for the hot-pressed material are shown in Fig. 3. The value of K_{IC} obtained at 800° C in an environment of argon plus water vapour was 4.07 MN m$^{-3/2}$, the same as that obtained at low temperature [6]. The value of the stress intensity exponent for the data shown at 600° C, ~110, is in good agreement with the results of Evans and Lange [7], and similar to the value obtained for moisture-induced stress corrosion at room temperature [6].

The appearance of region II in this investigation is the first time plateau behaviour has been reported in this material accompanied by a small slope in region I at these temperatures. Evans and Lange [7] reported region I behaviour and a slope of 21 for hot-pressed silicon carbide at 1400° C. The region I slope in the present investigation is 16. However, at 1400° C the small slope is attributed to crack propagation by plastic deformation at the grain boundaries, a mechanism which probably does not operate at the low temperatures studied in this investigation.

Thermodynamic calculations shown in Table III indicate that for all environments and temperatures investigated, the partial pressure of oxygen available for oxidation in the system is greater than the equilibrium partial pressure of oxygen for Equation 4, assuming an extreme upper limit for the partial pressure of CO of 1 atm., indicating that oxidation will occur. The equilibrium partial pressures in Table III are probably overestimates since the partial pressure of CO in the system is probably much less than 1 atm.

The data presented for 800° C indicate that, at

TABLE III Partial pressures of oxygen in the test ambients and equilibrium partial pressures of oxygen calculated from the ΔG°_Rs for $SiC_{(s)} + 3/2\ O_{2(g)} = SiO_{2(s)} + CO_{(g)}$, $K = P_{CO}/(P_{O_2})^{3/2}$.

Temperature (° C)	Input environment	ΔG°_R (cal mol^{-1})	Equilibrium P_{O_2} (atm) (assuming P_{CO} = 1 atm)	Available P_{O_2} (atm)
600	Ar + 0.3 vol% H_2O	−199 563	6.13×10^{-34}	5.09×10^{-7}
750	Ar + 0.3 vol% H_2O	−196 813	1.05×10^{-28}	7.15×10^{-7}
800	Ar + 1 vol% SO_2	−195 938	2.5×10^{-27}	5.008×10^{-7}
800	Ar + 0.3 vol% H_2O	−195 938	2.5×10^{-27}	1.04×10^{-6}
800	Ar + 1 vol% O_2	−195 938	2.5×10^{-27}	2.995×10^{-3}
800	Ar	−195 938	2.5×10^{-27}	5.0×10^{-7}
850	Ar + 0.3 vol% H_2O	−195 038	4.92×10^{-26}	1.75×10^{-6}

least within the precision of the calculations, the stress-corrosion mechanism is independent of the partial pressure of oxygen. This result suggests that if stress-corrosion occurs by an oxidation mechanism, the mechanism is operative as long as the partial pressure of oxygen in the ambient exceeds the equilibrium partial pressure of oxygen for oxidation of silicon carbide. These results coupled with the TGA data for the hot-pressed and direct-bonded materials indicate that the slow crack growth process is unrelated to the parabolic diffusion-controlled oxidation regime. One is led to the speculation that the crack growth process is controlled by the interface reaction rate controlled regime of oxidation in which the reaction rate is not much affected by the partial pressures at these very high values relative to the equilibrium partial pressures. However, since the cracks propagate intergranularly in this material, it is possible that the slow crack growth is controlled by a reaction of the atmosphere with a grain-boundary phase or by the intrinsic mechanical properties of this phase as suggested for the 1400° C behaviour [7]. More detailed studies are required to unequivocally establish the operative mechanisms. The stress corrosion behaviour indicated in Fig. 3 does not depend on the water content of the atmosphere indicating that moisture-induced stress-corrosion plays a secondary role, if any.

The magnitude of region II at these elevated temperatures is apparently not sensitive to the oxygen partial pressure. Regions II diminishes and is shifted to higher velocities with increasing temperatures sugesting that, as the temperature is increased the delivery rate of the corrosive species to the crack tip increases, if stress-corrosion is the operative mechanism. The result is that the crack must reach a higher velocity before delivery of the stress-corrosive species is rate-limiting. Also, a higher velocity must be reached before these species can no longer be delivered to the propagating crack and purely mechanical fracture governs the crack growth rate.

Fracture in the hot-pressed material was primarily intergranular. Fracture surfaces obtained at elevated temperatures were qualitatively indistinguishable from those obtained at low temperatures in relatively dry environments [6], indicating that the intergranular fracture is a result of the fine grain size, and that the stress-corrosion mechanism operating via the grain boundaries does not alter the type of fracture observed.

4. Conclusions

The direct-bonded silicon carbide exhibited unstable crack propagation and arrest behaviour in all environments and at all temperatures investigated even though the material exhibited considerable weight gain because of oxidation. It is thought that the large grain size, relative to specimen dimensions in the material used in this study, prohibited the observation of continuous sub-critical crack growth.

The hot-pressed silicon carbide exhibited slow crack growth at elevated temperatures in SO_2, H_2O, and O_2 containing ambients. It is suggested that the mechanism of slow crack growth is stress corrosion via the oxidation reaction and is operative as long as the available partial pressure of oxygen is in excess of the equilibrium partial pressure of oxygen for the oxidation of silicon carbide to SiO_2.

Acknowledgements

The authors gratefully acknowledge the financial support of the U.S. Army Research Office.

References

1. S. M. WIEDERHORN, A. G. EVANS and D. E. ROBERTS, in "Fracture Mechanics of Ceramics", Vol. 2, edited by R. C. Bradt, D. P. H. Hasselman, and F. F. Lange, Proceedings of the Symposium on the Fracture Mechanics of Ceramics, University Park, Pennsylvania, (1973), 829.
2. S. M. WIEDERHORN, *J. Amer. Ceram. Soc.* **50** (1967) 407.
3. S. M. WIEDERHORN and L. H. BOLTZ, *ibid.* **53** (1970) 543.
4. A. G. EVANS, *J. Mater. Sci.* 7 (1972) 1137.
5. D. P. WILLIAMS and A. G. EVANS, *J. Testing and Evaluation* 1 (1973) 264.
6. K. D. McHENRY, T. M. YONUSHONIS and R. E. TRESSLER, *J. Amera. Ceram. Soc.* **59** (1976).
7. A. G. EVANS and F. F. LANGE, *J. Mater. Sci.* **10** (1975) 1659.
8. G. G. TRANTINA and C. A. JOHNSON, *J. Amer. Ceram. Soc.* **58** (1975) 344.
9. J. E. RESTALL and C. R. GOSTELOW, *Proc. Brit. Ceram. Soc.* **22** (1973) 89.
10. M. L. TORTI, R. A. ALLIEGRO, M. E. WASHBURN, D. W. RICHERSON and G. Q. WEAVER, *ibid.* **22** (1973) 129.
11. F. F. LANGE, *J. Amer. Ceram. Soc.* **53** (1970) 290.
12. J. W. EDINGTON, D. J. ROWCLIFFE and J. L. HENSHALL, *P.M.I.* 7 (1975) 82.
13. D. W. RICHERSON, *Amer. Ceram. Soc. Bull.* **52** (1973) 560.
14. G. Q. WEAVER and B. A. OLSON, in "Silicon Carbide – 1973", edited by R. C. Marshall, J. W. Faust, Jun. and C. E. Ryan, Proceedings of the 3rd

International Conference on Silicon Carbide, Miami Beach, Florida (1973) p. 367.
15. M. G. ROGERS, in "Special Ceramics – 5", edited by P. Popper, Proceedings of the 5th Symposium on Special Ceramics (British Ceramic Research Association, Stoke-on-Trent, 1970 p. 87.
16. S. C. SINGHAL, in "Ceramics for High Performance Applications", edited by J. J. Burke, A. E. Gorum and R. N. Katz, Proceedings of the 2nd Army Materials Technology Conference, Hyannsis, Mass. (1973) p. 533.
17. K. M. NAIR, W. B. WHITE and R. ROY, *J. Amer. Ceram. Soc.* 48 (1965) 52.
18. E. FITZER and R. EBI, in "Silicon Carbide – 1973", edited by R. C. Marshall, J. W. Faust, and C. E. Ryan, Proceedings of the 3rd International Conference on Silicon Carbide, Miami Beach, Florida (1973) p. 320.
19. S. LIN, *J. Amer. Ceram. Soc.* 58 (1975) 271.

Received 16 June and accepted 22 October 1976.